JOURNAL OF VIROLOGY, Feb. 1993, p. 989–996
0022-538X/93/020989-08$02.00/0

Vol. 67, No. 2

RNA-Stimulated NTPase Activity Associated with Yellow Fever Virus NS3 Protein Expressed in Bacteria

PAUL WARRENER, JAMES K. TAMURA, AND MARC S. COLLETT*

MedImmune, Inc., 35 West Watkins Mill Road, Gaithersburg, Maryland 20878

Received 29 September 1992/Accepted 9 November 1992

The nonstructural protein NS3 of the prototypic flavivirus, yellow fever virus, was investigated for possession of an NTPase activity. The entire NS3 protein coding sequence and an amino-terminal truncated version thereof were engineered into *Escherichia coli* expression plasmids. Bacteria harboring these plasmids produced the expected polypeptides, which upon cell disruption were found in an insoluble aggregated material considerably enriched for the NS3-related polypeptides. Solubilization and renaturation of these materials, followed by examination of their ability to hydrolyze ATP, revealed an ATPase activity present in both the full-length and amino-terminal truncated NS3 preparations but not in a similarly prepared fraction from *E. coli* cells engineered to express an unrelated polypeptide. The amino-terminal truncated NS3 polypeptide was further enriched to greater than 95% purity by ion-exchange and affinity chromatography. Throughout the purification scheme, the ATPase activity cochromatographed with the recombinant NS3 polypeptide. The enzymatic activity of the purified material was shown to be a general NTPase and was dramatically stimulated by the presence of particular single-stranded polyribonucleotides. These results are discussed in view of similar activities identified for proteins of other positive-strand RNA viruses.

Amino acid sequence motifs conserved among proteins with similar known activities have been used to predict functions of uncharacterized polypeptides. Such data base sequence comparisons have identified several conserved motifs in proteins either demonstrated or postulated to be capable of nucleoside triphosphate (NTP) binding and hydrolysis and of nucleic acid unwinding (4, 5, 7, 13). This so-called D-E-A-D protein superfamily has members from both prokaryotic and eukaryotic cells as well as from numerous DNA and RNA virus groups. Proteins in this family play various roles in biochemical processes, including translation, transcription, recombination, and replication (22, 26). A number of these proteins have been experimentally demonstrated to possess NTP-dependent, nucleic acid-stimulated DNA (3, 14, 16, 21) or RNA (2, 6, 11, 17, 19, 20, 23) unwinding activity.

For the positive-strand RNA viruses, such putative NTP ase/RNA helicase proteins have been classified into three groups: alphavirus-like (e.g., nsP2-like proteins), picornavirus-like (e.g., 2C-like proteins), and polypeptides containing NTP-binding motifs similar to those encoded by the potyvirus-pestivirus-flavivirus groups (5, 12) (Fig. 1A). Among this last class of putative NTPases/helicases, biochemical data on polypeptides containing these NTP-binding motifs that substantiate the computer-based predictions of enzymatic activities are emerging. Laín and coworkers showed that the plum pox potyvirus CI protein isolated from virus-infected tobacco leaves copurified with a nucleic acid-stimulated ATPase activity (10) and further demonstrated the purified protein possessed an RNA helicase activity (11). Wengler and Wengler (27) demonstrated that a carboxy-terminal proteolytic segment of the NS3 protein purified from West Nile flavivirus (WNV)-infected baby hamster kidney (BHK) cells possessed a single-stranded RNA-stimulated NTPase activity. Finally, we recently established that the bovine viral diarrhea virus pestivirus p80 protein, purified from insect cells infected with a recombinant baculovirus, is associated with a single-stranded RNA-stimulated NTPase activity (25).

Here, we report on the engineered expression in *Escherichia coli* of a carboxy-terminal portion of the yellow fever flavivirus (YFV) NS3 protein, as well as the complete NS3 protein, and show that both recombinant polypeptides exhibit single-stranded RNA-stimulated NTPase activity. Initial enzymologic characterization of the purified NS3 NTP ase activity is presented. These characteristics for the YFV enzyme are compared with data on the NTPase activities of other positive-strand RNA viruses.

MATERIALS AND METHODS

Recombinant DNA techniques and expression cloning in *E. coli*. In general, all recombinant DNA and cloning procedures were carried out by standard methods (9, 15). For engineering the expression of the full-length YFV NS3 protein, specific primers were used to amplify by the polymerase chain reaction (PCR) a 1,869-bp fragment encompassing the complete 623-amino-acid coding region of NS3 from plasmid pYFM3.5 (graciously provided by C. Rice, Washington University, St. Louis, Mo.). The 5′ (N-terminal) primer was 5′-GGTGGAAGCTTGCAGATCTGGCCATGGGTGAT GTCTTGTGGGATATTCCC-3′ and incorporated an ATG codon at the position of the first amino acid of the NS3 protein, replacing the natural AGT serine codon. The 3′ (C-terminal) primer was 5′-GCTCCCGGGTCACCTCCTACCT TCAGCAAAC-3′ and incorporated a translation termination codon immediately following the codon of the last amino acid (residue 623) of the mature NS3 protein. The nucleotides in large capitals indicate YFV positive-strand or complementary-strand sequences. By using the *Hin*dIII and *Sma*I sites in the primers (double underlines), the resulting PCR fragment was restricted, and the ends were made blunt with Klenow DNA polymerase and dNTPs. The fragment was cloned into the appropriately phased site within the multiple cloning site of the bacterial expression vector

* Corresponding author.

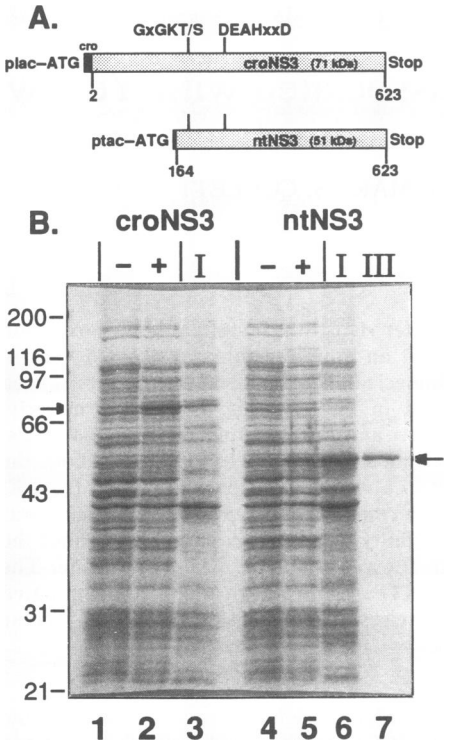

FIG. 1. Bacterial expression of the YFV NS3 protein. (A) Schematic representation of the protein coding domains engineered into *E. coli* expression vectors. The relative positions of the promoters, initiation and stop codons, encoded NS3 amino acids, and the NTP-binding motifs A (GxGKT/S) and B (DEAHxxD) (5) are indicated. The solid box (cro) preceding the croNS3 gene represents the sequence coding for 23 amino acids of the Cro protein fused to the NS3 gene. The small solid box preceding the ntNS3 gene represents vector-derived sequences encoding four amino acids (see Materials and Methods). (B) SDS-PAGE analysis of extracts of *E. coli* cells harboring plasmids pcroNS3 or pntNS3. Whole-cell SDS lysates of cultures either uninduced (−) or IPTG induced (+) were prepared and subjected to SDS-PAGE and Coomassie blue staining. Lanes 1 and 2 show cells harboring pcroNS3; lanes 4 and 5 show pntNS3-containing cells. Crude aggregate materials, solubilized and dialyzed as described in Materials and Methods (fraction I), were prepared from induced cultures of cells harboring pcroNS3 and pntNS3 and are shown in lanes 3 and 6, respectively. Material in the pooled and dialyzed fractions from the poly(U)-Sepharose column ntNS3 protein peak (fraction III) is shown in lane 7. Positions of the croNS3 (71-kDa) and ntNS3 (51-kDa) proteins are indicated by arrows at left and right, respectively. Molecular mass standards, in kilodaltons, are indicated at the left.

p346-2. Vector p346-2 is a derivative of the previously described expression plasmid pTC413 (9). Briefly, p346-2 consists of a *lac* promoter, the ribosome binding site, and the first 23 codons of the bacteriophage lambda *cro* gene followed by multiple cloning sites and the *rrnB* T1 transcription terminator. The resulting construct, termed pcroNS3, directed the synthesis of a 647-amino-acid croNS3 fusion polypeptide.

For expression of an N-terminal truncated version of the NS3 protein (ntNS3), a similar approach was used. The 5′ and 3′ PCR primers used to amplify a 1,380-bp fragment from plasmid pYFM3.5 were 5′-GCCCCATGGAAGCTTCGT GTCCGCCATATCCCAG-3′ and 5′-CGCCCCGGGCTACCTCC TACCTTCAGCAAACTT-3′, respectively. They encompass the sequences encoding amino acids 164 to 623 of the NS3 protein. The resultant PCR fragment, restricted at the *Hin*dIII and *Sma*I sites and filled in by Klenow polymerase, was inserted into the *Hpa*I site of bacterial expression vector p469/1. This vector consists of the *tac* promoter, the *cro* ribosome binding site, a four-codon ATG-initiated sequence followed by a *Hpa*I restriction site, and the *rrnB* T1 transcription terminator. The resulting construct, termed pntNS3, directed the synthesis of the 464 carboxy-terminal amino acids of the NS3 protein.

A third bacterial expression plasmid, pcroVP1-227M (18), encoding a portion of the minor capsid protein of human parvovirus B19, was used as a negative control in several experiments.

Expression plasmids pcroNS3, pntNS3, and pcroVP1-227M were transformed into *E. coli* W3110 (15) containing a stable F′ *lacI*^{q} episome. Upon induction with 1 mM isopropyl-β-D-thiogalactopyranoside (IPTG), cultures harboring these plasmids expressed high levels of polypeptides of the expected sizes (71, 51, and 32 kDa, respectively).

Extraction and renaturation of recombinant polypeptides. Log-phase cultures (50 ml) of transformed bacteria were adjusted to 1 mM IPTG and grown 3 h at 37°C. Harvested cells were resuspended in 4 ml of GET buffer (50 mM glucose, 10 mM EDTA, 25 mM Tris-HCl [pH 8.0]) containing 250 μg of lysozyme per ml and incubated 20 min at 4°C, at which time the suspension was adjusted to 1% Triton X-100 and sonicated extensively. $MgCl_2$ and DNase I were added to 20 mM and 10 μg/ml, respectively. Suspensions were incubated for an additional 20 min at 24°C and were then layered onto a 0.75-ml cushion of 35% sucrose–0.5% Triton X-100 in STE buffer (150 mM NaCl, 10 mM Tris-HCl [pH 7.4], 1 mM EDTA). Following centrifugation at 4°C for 30 min at 30,000 × *g*, pelleted aggregates were resuspended in 2 ml of a solution consisting of 100 mM glycine-NaOH (pH 10.5), 1% Triton X-100, and 2 mM EDTA and incubated 60 min at 4°C. The materials were repelleted by centrifugation at 10,000 × *g* for 10 min and were then resuspended in 2 ml of solubilization buffer (5 M guanidine-HCl, 50 mM Tris-HCl [pH 8.0], 1 mM EDTA) by brief sonication. After a 60 min incubation at 4°C and clearing of any insoluble material by centrifugation for 20 min at 20,000 × *g*, the solubilized proteins were renatured by dialysis against 500 volumes of 0.5 M guanidine-HCl–50 mM Tris-HCl [pH 8.0]–1 mM EDTA–1 mM dithiothreitol–20% glycerol overnight at 4°C. The dialysates were cleared and then dialyzed against buffer A (25 mM *N*-2-hydroxyethylpiperazine-*N*′-2-ethanesulfonic acid [HEPES; pH 7.4], 50 mM KCl, 1 mM EDTA, 0.02% 2-mercaptoethanol, 0.01% Triton X-100, 50% glycerol) for at least 6 h at 4°C. These final dialysates were again cleared and then stored at −20°C. The materials at this stage will be referred to as fraction I.

Purification of the ntNS3 protein. All chromatographic procedures were performed at 4°C. Fraction I of the ntNS3 preparation (1 to 2 ml) was diluted with 9 volumes of buffer B (25 mM HEPES [pH 7.4], 1 mM EDTA, 0.02% 2-mercaptoethanol, 0.05% Triton X-100, 10% glycerol) containing 50 mM NaCl. This solution was loaded onto a 2-ml-bed-volume Q-Sepharose Fast Flow column equilibrated in the same buffer. Proteins were eluted with a 40-ml linear gradient of 50 to 500 mM NaCl in buffer B. Fractions (1.2 ml) were collected and analyzed by both the standard ATPase assay (see below) and sodium dodecyl sulfate (SDS)-containing polyacrylamide gel electrophoresis (PAGE). Peak ntNS3 protein-containing fractions were pooled and dialyzed

against buffer A overnight at 4°C and then stored at −20°C. This material represents fraction II.

Fraction II was diluted with 9 volumes of buffer B containing 50 mM NaCl and loaded onto a 2-ml-bed-volume poly(U)-Sepharose CL-6B column equilibrated in buffer B containing 50 mM NaCl. The proteins were eluted with a 40-ml gradient of 50 to 500 mM NaCl in buffer B, and fractions (1.2 ml) were analyzed by the standard ATPase assay and SDS-PAGE. Peak ntNS3 protein-containing fractions were pooled, dialyzed against buffer A overnight at 4°C, and then stored at −20°C. This material represents fraction III.

NTPase assays. Two assays were used to measure NTPase activity. Standard analytical ATPase assays were carried out in a final volume of 10 μl containing 50 mM Tris-HCl (pH 8.0), 10 mM NaCl, 2.5 mM $MgCl_2$, 200 μM [α-^{32}P]ATP (2.5 Ci/mmol; Amersham), and 1 to 2 μl of protein sample. Reactions were incubated at 24°C for 60 min, at which time they were terminated by the addition of EDTA to a final concentration 20 mM. Reaction products were analyzed by thin-layer chromatography (TLC). One-half microliter of the reaction mixture was spotted onto plastic-backed polyethyleneimine-cellulose sheets (Baker) and developed by ascending chromatography in 0.375 M potassium phosphate (pH 3.5). The sheets were dried and exposed to X-ray film.

The second NTPase assay involved a continuous spectrophotometric assay that coupled the hydrolysis of NTP (dNTP) to the oxidation of NADH (24). Comparison studies demonstrated the equivalence of results obtained in this assay and in the [α-^{32}P]NTP (dNTP)/TLC assay. Except where indicated in figure legends, standard coupled enzyme reaction mixtures contained 50 mM morpholinepropanesulfonic acid (MOPS)-KOH (pH 6.5), 2.5 mM $MgCl_2$, various concentrations of NTP (dNTP), 1.95 mM phosphoenolpyruvate, NADH (100 μg/ml), pyruvate kinase (100 μg/ml; Boehringer Mannheim), lactate dehydrogenase (25 μg/ml; Boehringer Mannheim), and 2 to 6 μl of enzyme preparation in buffer A in a final volume of 100 μl. The coupling enzymes used in this system are active over a broad range of pH, divalent cation, and salt conditions (8, 24). After mixing, reaction mixtures were immediately added to a microcuvette at 24°C, and continuous spectrophotometric readings were taken at 340 nm for 10 to 20 min. The steady-state rate of NTP (dNTP) hydrolysis was determined from the slope of the line of decreasing absorbance. This coupled assay was used for enzyme kinetic analyses with all NTP and dNTP substrates except dCTP and dTTP. As dCDP and dTDP are poor substrates for the pyruvate kinase reaction in the coupled system (8), kinetic measurements with these substrates were carried out by the [α-^{32}P]dNTP/TLC assay. Resolution of radiolabeled dCDP/dCTP and dTDP/dTTP was achieved on polyethyleneimine-cellulose sheets by TLC, using 0.15 M KH_2PO_4 (pH 3.5) and 0.1 M KH_2PO_4 (pH 3.5), respectively. Enzymatic activity was quantified by liquid scintillation counting of the regions of the plastic sheets corresponding to dNDP and dNTP for each reaction and determining the percent conversion of dNTP to dNDP.

RESULTS

Expression of the YFV NS3 protein in bacteria. To provide an abundant source of flavivirus NS3 protein for biochemical studies relating to its putative NTPase and RNA helicase activities, we engineered the coding sequence for the YFV NS3 protein into *E. coli* expression vectors. Two vectors were constructed, one in which the entire NS3 coding sequence was included and a second in which the amino-terminal portion of the protein had been deleted. This latter construct was considered for two reasons. First, we had observed difficulties with the solubility of the whole NS3 protein from mammalian cells infected with YFV and from insect cells infected with an NS3-expressing recombinant baculovirus (unpublished observations). Second, Wengler and Wengler have shown that a subtilisin-generated fragment encompassing the carboxyl-terminal 75% of the WNV NS3 prepared from virus-infected BHK cells was soluble and possessed NTPase activity (27).

The two constructs are schematically represented in Fig. 1A. Plasmid pcroNS3 contains the entire coding region of the YFV NS3 protein fused at its amino terminus to the first 23 amino acids of the bacteriophage lambda cro protein and is terminated at its natural carboxy terminus by an engineered translational termination codon. Transcription in pcroNS3 is directed by the *lac* promoter. In the second construct, plasmid pntNS3, the *tac* promoter controls transcription of RNA containing an open reading frame in which four vector-derived amino acids are fused to amino acid 164 of the NS3 coding region. The NTP-binding motifs lie downstream of this position (Fig. 1A). The open reading frame then continues to an engineered termination codon immediately following the last codon of the NS3 protein.

E. coli harboring these plasmids showed the induction-specific production of new proteins of the expected sizes. Upon induction with IPTG of pcroNS3-containing bacteria, a new protein of about 71 kDa appeared (Fig. 1B, lanes 1 and 2). Similarly, pntNS3-containing *E. coli* expressed a new 51-kDa polypeptide upon addition of IPTG to the culture (Fig. 1B, lanes 4 and 5). In both cases, the polypeptides were specifically reactive in a Western immunoblot assay with an anti-NS3 peptide antiserum (data not shown). Both proteins were expressed at relatively high levels (approximately 8% of total cell protein) and upon cell disruption were present in an insoluble aggregated form.

Detection of an ATPase activity in crude preparations of *E. coli*-produced croNS3 and ntNS3. Since the NS3 polypeptides were enriched severalfold in the crude aggregate preparations, we evaluated these materials for a YFV-specific ATPase activity. The crude aggregate materials were solubilized in guanidine-HCl and then renatured by dialysis (see Materials and Methods section). The dialyzed materials (termed fraction I; Fig. 1B, lanes 3 and 6) were then tested for ATPase activity. To serve as an NS3 protein-negative control, material was prepared in an identical fashion from *E. coli* cells engineered to express an unrelated polypeptide (croVP1-227M).

Comparable amounts of fraction I protein prepared from each of the three recombinant *E. coli* preparations were evaluated for ATPase activity in two assays. As the ATPase activity of the WNV NS3 proteolytic fragment had previously been shown to be stimulated by the homopolymer poly(A) (27), we performed these assays both in the absence and in the presence of poly(A). As shown in Fig. 2A, in the [α-^{32}P]ATP/TLC assay, both the croNS3 and ntNS3 fraction I preparations contained an ATPase activity that was significantly stimulated upon addition of poly(A). In the control preparation (croVP1-227M), only a trace level of ATPase activity was detectable with or without added poly(A) (Fig. 2A). Similar results were obtained in the coupled spectrophotometric assay: only the fraction I materials from croNS3 and ntNS3 cells showed significant ATPase activity, and these activities were dramatically enhanced by the addition of poly(A) (Fig. 2B).

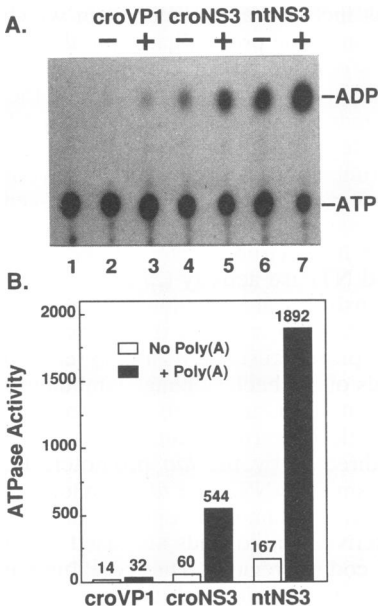

FIG. 2. ATPase activity in fraction I from croVP1-227M, croNS3, and ntNS3 in the absence and presence of poly(A). ATPase measurements on fraction I materials were performed in either the [α-^{32}P]ATP/TLC assay (A) or the coupled enzyme assay (B). Coupled reaction mixtures contained 50 mM Tris-HCl (pH 8.0), 10 mM NaCl, 0.35 mM ATP, 2.5 mM $MgCl_2$, and, when present, 1 mM poly(A). The ATPase activities determined in the coupled reactions are presented as picomoles of ATP hydrolyzed per minute per microgram of total fraction I protein.

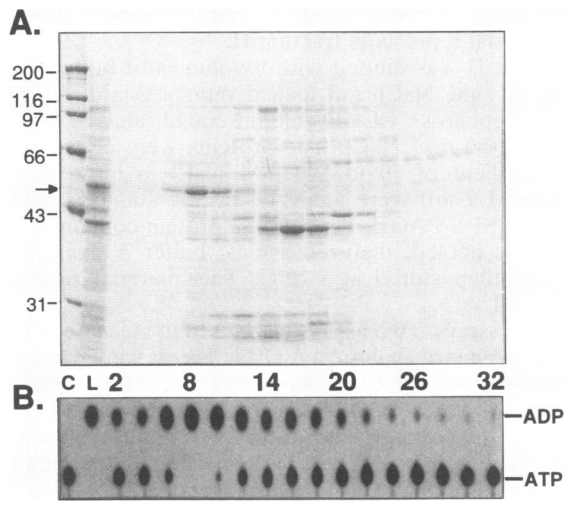

FIG. 3. Chromatography of ntNS3 fraction I on Q-Sepharose. Fraction I material (A, lane L) was applied to a Q-Sepharose Fast Flow column as described in Materials and Methods. Proteins were eluted with a 50 to 500 mM NaCl gradient, and even-numbered fractions from 2 through 32 were analyzed by SDS-PAGE and Coomassie blue staining (A). The same column fractions were also evaluated in the standard [α-^{32}P]ATP/TLC assay (B). Molecular mass standards (A) and the buffer-only ATPase reaction (B) are shown in lane C. Sizes are indicated in kilodaltons.

Purification of the ntNS3 protein. The data presented above indicate that the observed poly(A)-stimulated ATPase activities were specific to *E. coli* harboring the pcroNS3 and pntNS3 plasmids. To more directly established that this activity was associated with the recombinant YFV NS3 sequences, we undertook the biochemical purification of the ntNS3 polypeptide. We focused our efforts on the ntNS3 protein because it was more highly enriched and quite active in fraction I and exhibited better solubility characteristics than did the croNS3 protein.

The crude ntNS3 protein preparation was first subjected to anion-exchange chromatography. Fraction I was applied to a column of Q-Sepharose. After the column was washed with loading buffer, proteins were eluted with a linear gradient of NaCl. Proteins in even-numbered gradient fractions were then analyzed by gel electrophoresis. Figure 3A shows the protein fractionation provided by this column. The ntNS3 protein eluted in a peak centered at fraction 8, representing an NaCl concentration of approximately 150 mM. ATPase activity was also monitored across the Q-Sepharose column. The peak of enzymatic activity appeared to coelute with the Coomassie blue-stained ntNS3 polypeptide (Fig. 3B). The peak ntNS3 protein-containing fractions from this column were pooled and dialyzed against buffer A to yield fraction II.

Fraction II was then subjected to chromatography on poly(U)-Sepharose as described in Materials and Methods. Following application of fraction II, the column was washed with loading buffer, and proteins were eluted with a linear gradient of NaCl. Figure 4A shows the Coomassie blue-stained protein elution profile for this column. Elution of the ntNS3 polypeptide peaked at fraction 16, corresponding to

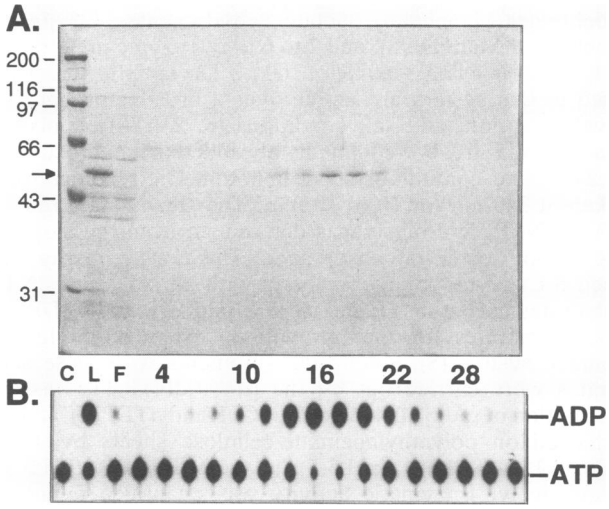

FIG. 4. Chromatography of ntNS3 fraction II on poly(U)-Sepharose. Peak ntNS3 protein-containing fractions from the Q-Sepharose column were pooled and dialyzed (fraction II material; A, lane L) and then applied to a poly(U)-Sepharose column as described in Materials and Methods. After loading and collection of the column flowthrough material, bound proteins were eluted with a 50 to 500 mM NaCl gradient. The column flowthrough fraction (lane F) and even-numbered fractions from 2 through 32 of the salt gradient elution were analyzed by SDS-PAGE and Coomassie blue staining (A). The same column fractions were also evaluated in the standard [α-^{32}P]ATP/TLC assay (B). Molecular mass standards (A) and the buffer-only ATPase reaction (B) are shown in lane C. Sizes are indicated in kilodaltons.

TABLE 1. Summary of the purification of ntNS3

Fraction	Total protein[a] (μg)	ATPase sp act[b]	Fold enrichment		ntNS3 protein	
			ATPase	ntNS3	% Purity[c]	% Yield
Starting extract	10,000	—[d]	—	1	8	100
Fraction I (crude dialysate renatured)	1,260	166	1	2	19	30
Fraction II (Q-Sepharose)	466	909	6	6	50	29
Fraction III [poly(U)-Sepharose]	74	1,353	8	12	96	9

[a] Determined by the bicinchoninic acid assay using bovine serum albumin as a standard.
[b] Determined by the coupled enzyme assay performed at pH 8.0 and presented as picomoles of ATP hydrolyzed per minute per microgram of total protein.
[c] Estimated by scan analysis of tracks of Coomassie blue-stained SDS-polyacrylamide gels.
[d] —, NS3-specific ATPase activity could not be determined in this fraction.

an NaCl concentration of approximately 270 mM. Measurement of ATPase activity across the poly(U) column gradient fractions revealed a peak of activity also centered at fraction 16 (Fig. 4B). The peak ATPase/ntNS3 protein-containing fractions were pooled and dialyzed against buffer A to yield fraction III. Gel analysis of this final dialyzed material showed the ntNS3 polypeptide to be nearly homogeneous (Fig. 1B, lane 7). By scanning analysis of the Coomassie blue-stained gel, we estimate the purity of the ntNS3 fraction III to be greater than 95%. A summary of the purification of the ntNS3 protein-associated ATPase activity is presented in Table 1.

Characterization of the NTPase activity. The fact that the ATPase activity cochromatographed with the ntNS3 polypeptide across both the Q-Sepharose and poly(U)-Sepharose columns strongly suggests the ATPase activity is a property of the ntNS3 polypeptide. We went on to more fully characterize the ntNS3-associated ATPase activity in the fraction III preparation. Initially, we determined the optimal reaction conditions for enzymatic activity. Using the coupled enzyme ATPase assay, we determined the optima for reaction pH and for divalent cation (Mg^{2+}) and monovalent cation (K^+) concentrations, using ATP as the substrate. Since the ntNS3 ATPase activity was stimulated by the homopolymer poly(A), these optima were determined both in the absence and in the presence of poly(A).

In the absence of poly(A), the ntNS3 ATPase activity was largely unaffected by pH over the range tested (pH 5.5 to 9.0; Fig. 5A). However, an optimum for the ATPase activity in the presence of poly(A) was observed at pH 6.5. The ATPase activity was absolutely dependent on the presence of a divalent cation; omission of $MgCl_2$, or addition of EDTA to the complete reaction mixture prior to addition of the enzyme, completely prevented the hydrolysis of [α-^{32}P]ATP in the TLC assay (data not shown). Under three different reaction conditions (50 mM MOPS-KOH buffer [pH 6.5], 50 mM MOPS-KOH buffer [pH 6.5] plus 100 mM KCl, and 100 mM potassium acetate [pH 7.3]) in the absence of poly(A), the ATPase activity was largely unaffected by the concentration of $MgCl_2$ between 0.5 and 10 mM (Fig. 5B). In the presence of poly(A), the ATPase activity in the MOPS-buffered reaction plateaued at 2.5 mM $MgCl_2$. However, in this reaction mixture, activity could not be measured at $MgCl_2$ concentrations greater than 5 mM because of the formation of a precipitate upon addition of poly(A). When poly(A)-containing reactions were performed in MOPS buffer supplemented with 100 mM KCl, precipitate formation was not observed at any $MgCl_2$ concentration. Under these conditions, the optimum ATPase activity occurred at 1 mM $MgCl_2$ and decreased with increasing cation concentration (Fig. 5B). When reactions were performed in 100 mM potassium acetate (pH 7.3) in the presence of poly(A), the ATPase activity profile over the range of $MgCl_2$ concentrations mirrored that seen for the MOPS/KCl reactions. However, in the latter two reactions, the maximal poly(A)-stimulated ATPase activity was only 55 to 65% of that observed in the MOPS-buffered reaction lacking KCl.

These data suggested that the poly(A)-stimulated ATPase activity was inhibited by potassium salts. In Fig. 5C, we show this is indeed the case. The ATPase activity in the presence of poly(A) was significantly inhibited with increasing KCl in the MOPS-buffered reaction containing 2.5 mM $MgCl_2$. In contrast, in the absence of poly(A), the ntNS3 ATPase activity was unaffected by the concentration of KCl in the reaction mixture (Fig. 5C). Similar results were seen with NaCl (data not shown). Since the poly(A)-stimulated ATPase activity was highest in reactions consisting of 50 mM MOPS-KOH (pH 6.5)–2.5 mM $MgCl_2$, these conditions were selected for all subsequent ATPase measurements.

Using these optimized reaction conditions, we investigated the effect of a variety of polynucleotides on the YFV NS3 ATPase activity (Table 2). The ntNS3 ATPase activity was stimulated to the greatest degree (8- to 14-fold) by addition of the homopolymers poly(A), poly(C), and poly(U) and the single-stranded heteropolymer poly(ACU). Lower but still significant levels of activity stimulation (three to fourfold) were observed with several additional single-stranded ribo- and deoxyribo-homopolymers and the two duplex homopolyribonucleotides that were tested. However, since these duplex RNAs are made up of homopolymers that, when single stranded, were potent stimulators of activity, it is difficult to interpret the significance of these results. Duplex DNA did not enhance the ATPase activity (Table 2). Marginal or no stimulation was observed with poly(dA), poly(dC), and poly(G) (Table 2). The concentration of poly(A) required to achieve half-maximal stimulation of the ntNS3 ATPase activity was 0.4 μM (micromoles of nucleotide; data not shown).

The kinetics of ATP hydrolysis by the ntNS3 ATPase in the absence and presence of poly(A) was examined under the optimal reaction conditions. Lineweaver-Burk plots of the data obtained both with and without poly(A) were linear over the range of ATP concentrations tested (0.1 to 1.0 mM; data not shown), suggesting that only one class of ATP catalytic site is present on the enzyme. Determination of K_m and k_{cat} values from these plots showed that while the K_m for ATP was only minimally affected upon the addition of poly(A), a dramatic increase in k_{cat} was apparent (Table 3).

Finally, in addition to ATP, the ntNS3 fraction III enzyme was evaluated for its ability to hydrolyze other substrates. The ntNS3 enzyme effectively hydrolyzed a variety of NTPs (Table 3). The K_m values for all substrates, with or without

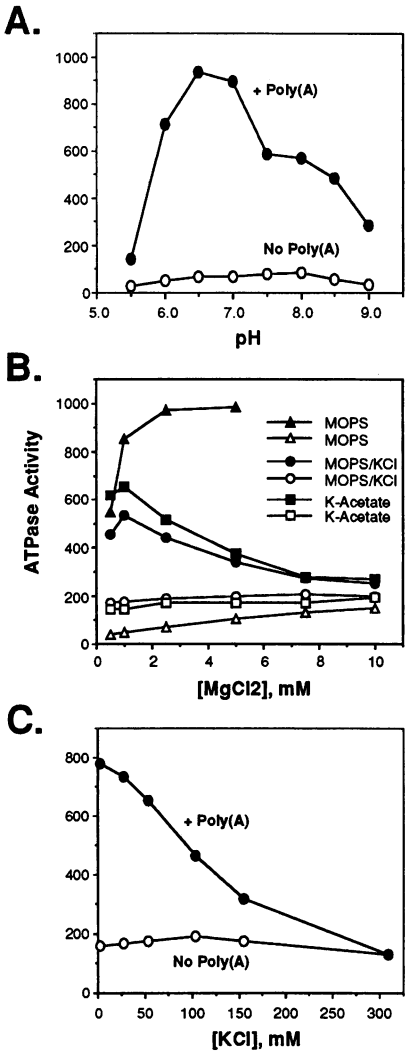

FIG. 5. Optimization of ntNS3 fraction III ATPase reaction conditions. Rates of ATP hydrolysis were determined in the coupled enzyme assay at 0.35 mM ATP as described in Materials and Methods. All activities are presented as picomoles of ATP hydrolyzed per minute per picomole of ntNS3 polypeptide. (A) The optimal pH of the ATPase activity was determined in 50 mM buffer at the indicated pH containing 2.5 mM $MgCl_2$, with and without 1 mM poly(A). Buffers were as follows: pH 5.5 and 6.0, morpholineethanesulfonic acid (MES)-HCl; pH 6.5 and 7.0, MOPS-KOH; pH 7.5 to 9.0, Tris-HCl. (B) The effect of varying the $MgCl_2$ concentration was determined under three reaction conditions: 50 mM MOPS-KOH (pH 6.5) (triangles), 50 mM MOPS-KOH (pH 6.5) containing 100 mM KCl (circles), and 100 mM potassium acetate (pH 7.3) (squares), in the absence (open symbols) or presence (closed symbols) of 0.25 mM poly(A). (C) The effect of varying the KCl concentration was determined in 50 mM MOPS-KOH (pH 6.5)–2.5 mM $MgCl_2$, with and without 0.5 mM poly(A).

poly(A), were quite similar, varying by only about two- to threefold. In the absence of RNA, it appeared that dNTPs, and in particular dTTP, were hydrolyzed more slowly than NTPs. The rates of hydrolysis (k_{cat}) of the different substrates were enhanced from 5- to 13-fold by the addition of poly(A). The ratio k_{cat}/K_m can be used to define the substrate specificity of an enzyme. Using this parameter, it appeared that in the presence of poly(A), the YFV NS3 NTPase prefers purine (either ribo- or deoxyribo-) triphosphates.

TABLE 2. Effects of polynucleotides on ntNS3 ATPase activity

Polynucleotide	ATPase activity[a]	Relative activity[b]
None	72	1.0
Poly(A)	1,007	14.0
Poly(C)	615	8.6
Poly(U)	573	8.0
Poly(I)	250	3.5
Poly(G)	41	0.6
Poly(ACU)	662	9.2
Poly(dA)	125	1.8
Poly(dC)	112	1.6
Poly(dU)	321	4.5
Poly(dI)	223	3.1
Poly(dT)	230	3.2
Poly(A) · poly(U)	305	4.2
Poly(I) · poly(C)	294	4.1
pUC9 DNA (linear)	102	1.4

[a] Coupled enzyme ATPase assays were performed at 24°C in a final volume of 100 μl containing 50 mM MOPS-KOH (pH 6.5), 2.5 mM $MgCl_2$, 0.35 mM ATP, 0.25 mM polynucleotide (concentrations were determined spectrophotometrically and are in millimoles of nucleotide base or base pair), and 0.96 pmol of ntNS3 fraction III polypeptide. All polynucleotides were obtained from Pharmacia LKB Biotechnology (Piscataway, N.J.). ATPase activity is expressed as picomoles of ATP hydrolyzed per minute per picomole of enzyme.

[b] The activity of the enzyme reaction without added polynucleotides was taken to be 1.0, and all other activity values were normalized to this value.

DISCUSSION

The data presented in this report on the YFV NS3 protein confirm the earlier observations of Wengler and Wengler regarding the WNV NS3 polypeptide (27). These workers showed that the protease subtilisin released a carboxy-terminal segment of the WNV NS3 protein from a membrane fraction of virus-infected BHK cells and that this soluble NS3 fragment copurified with a single-stranded RNA-stimulated NTPase (27). Here, we show by a genetic engineering approach that the YFV NS3 protein possesses a similar RNA-stimulated NTPase activity. The expression in bacteria of the carboxy-terminal portion of the YFV NS3 protein, as well as the complete NS3 protein, resulted in synthesis of recombinant YFV polypeptides exhibiting this enzymatic activity.

The characteristics of the two flavivirus enzymes appear quite similar. Both enzyme activities, in the absence of nucleic acids, were largely unaffected by various reaction conditions. However, the activities in the presence of poly(A) were quite sensitive to monovalent and divalent cation concentrations. Wengler and Wengler showed that the WNV NS3 ATPase was extremely sensitive to Mg^{2+} concentrations above 4 mM (27). Using the same reaction buffer (100 mM potassium acetate [pH 7.3]), we also observed inhibition of ATPase activity as the Mg^{2+} concentration was increased over 1 mM (Fig. 5B). By minimizing the K^+ concentration, however, we were able to obtain higher levels of activity at an optimum $MgCl_2$ concentration of 2.5 mM. Both the YFV and WNV enzymes have a broad specificity for nucleotide substrates; they hydrolyzed all NTPs and dNTPs tested. The YFV enzyme did, however, show a slight preference for ribo- and deoxyribo-purine triphosphates in the presence of poly(A) (Table 3).

The profiles of the relative effects of added nucleic acids

TABLE 3. Kinetic analyses of NTP and dNTP hydrolysis by the purified ntNS3 preparation[a]

Substrate	No poly(A)			With poly(A)		
	K_m (mM)	k_{cat} (mm^{-1})	k_{cat}/K_m	K_m (mM)	k_{cat} (mm^{-1})	k_{cat}/K_m
ATP	0.21	173	1,020	0.09	882	9,768
GTP	0.19	133	701	0.11	1,303	11,847
UTP	0.19	152	799	0.24	1,133	4,719
CTP	0.11	122	1,106	0.12	785	6,543
dATP	0.17	106	624	0.07	1,117	15,094
dGTP	0.20	100	499	0.12	1,247	10,391
dTTP	0.15	45	298	0.23	572	2,140
dCTP	0.09	96	359	0.09	540	6,280

[a] Values for K_m and k_{cat} were determined from Lineweaver-Burk plots of hydrolysis activity measured in the coupled enzyme assay or, in the cases of dCTP and dTTP, by the TLC assay. Reactions were conducted with NTP or dNTP concentrations varying between 0.10 and 1.0 mM in 50 mM MOPS-KOH (pH 6.5) at 24°C. The $MgCl_2$ concentration was maintained at 2.5 mM above the NTP/dNTP concentration. When included, the concentration of poly(A) was 0.5 mM.

on the ATPase activities of the two enzymes were quite similar. Poly(U) and poly(A) were potent stimulators of both enzymes. However, the YFV ATPase activity was also greatly enhanced by poly(C) and heteropolymeric single-stranded RNA, while WNV enzyme was only moderately enhanced by these nucleic acids. Interestingly, for both enzymes, poly(G) actually inhibited the activities slightly. Single- and double-stranded DNAs either were marginally stimulatory or had no effect at all on the ATPase activity of both enzymes.

Attempts to compare the specific activities of the two flavivirus enzymes are difficult and can be considered as only tentative at this time. For valid comparisons, the K_m values for the substrate for both enzymes must be known. In the case of the WNV NS3 enzyme, this value was not reported (27). However, superficially it appears the specific activities of the two enzymes may not differ drastically. For example, under the set of reactions conditions most similar (but not identical) between the two enzymes, the specific activities for ATP in the absence and presence of poly(A) were 174 and 518 pmol/min/pmol, respectively, for the YFV ntNS3 enzyme and were 37 and 500 pmol/min/pmol, respectively, for the WNV p50 NS3 enzyme. If such a comparison is accepted, it would indicate that our means for preparation of the *E. coli*-produced ntNS3 material, involving protein denaturation and refolding, was quite efficient. However, with the available information, we remain reserved about the validity of such comparisons of specific activities.

The flavivirus NS3 proteins are members of a group of positive-strand RNA virus putative NTPase/RNA helicases that also includes polypeptides from the potyviruses and pestiviruses (5, 12). From these latter groups, the viral proteins with the NTP-binding motifs have been demonstrated experimentally to possess RNA-stimulated NTPase activity. In the case of the plum pox potyvirus, the CI protein ATPase activity was stimulated by both poly(A) and poly(dA), with a half-maximal stimulatory concentration in the range of 3 μM (10), slightly higher than that for the YFV ntNS3 enzyme (0.4 μM). In contrast to the flavivirus and potyvirus enzymes, the pestivirus p80 NTPase activity was enhanced most by either poly(U) or poly(C) and was only minimally affected by poly(A) (25). The half-maximal stimulatory concentration for poly(U) was determined to be 2 μM for the pestivirus ATPase (25). For all enzymes of this group, the RNA-stimulated activities were sensitive to KCl, while the reactions in the absence of RNA were unaffected by salt.

The meaning and significance of these comparisons will require further study. Of particular relevance will be the thorough investigation of the template specificity and enzymologic characteristics of the RNA helicase activities presumed to be associated with these NTPases. The NS3 *E. coli* expression system described here provides an abundant source of material for such biochemical and enzymologic studies. Efforts to identify and investigate the predicted RNA helicase activity can now be pursued. This engineered expression system is also well suited for undertaking structure-function studies to explore the actual role of the NTP-binding motifs, as well as other conserved residues, in the enzymatic activities of this polypeptide.

ACKNOWLEDGMENTS

We thank Thomas O'Neill for construction of plasmid pcroNS3 and JoAnn Suzich for her interest in, and critical review of, this work.

REFERENCES

1. **Boehmer, P. E., and P. T. Emmerson.** 1992. The RecB subunit of the *Escherichia coli* RecBCD enzyme couples ATP hydrolysis to DNA unwinding. J. Biol. Chem. **267**:4981–4987.
2. **Ford, M. J., I. A. Anton, and D. P. Lane.** 1988. Nuclear protein with sequence homology to translation initiation factor eIF-4A. Nature (London) **332**:736–738.
3. **Geider, K., and H. Hoffmann-Berling.** 1981. Proteins controlling the helical structure of DNA. Annu. Rev. Biochem. **50**:233–260.
4. **Gorbalenya, A. E., A. P. Donchenko, V. Koonin, and V. M. Blinov.** 1988. A conserved NTP-motif in putative helicases. Nature (London) **333**:22.
5. **Gorbalenya, A. E., E. V. Koonin, A. P. Donchenko, and V. M. Blinov.** 1989. Two related superfamilies of putative helicases involved in replication, recombination, repair and expression of DNA and RNA genomes. Nucleic Acids Res. **17**:4713–4729.
6. **Hirling, H., M. Scheffner, T. Restle, and H. Stahl.** 1989. RNA helicase activity associated with human p68 protein. Nature (London) **339**:562–564.
7. **Hodgman, T. C.** 1988. A new superfamily of replicative proteins. Nature (London) **333**:22–23.
8. **Kayne, F. J.** 1973. Pyruvate kinase. Enzymes **8**:353–382.
9. **Keegan, K., and M. S. Collett.** 1986. Use of bacterial expression cloning to define the amino acid sequences of antigenic determinants on the G2 glycoprotein of Rift Valley fever virus. J. Virol. **58**:263–270.
10. **Laín, S., M. T. Martín, J. L. Riechmann, and J. A. García.** 1991. Novel catalytic activity associated with positive-strand RNA virus infection: nucleic acid-stimulated ATPase activity of the plum pox potyvirus helicase-like protein. J. Virol. **65**:1–6.
11. **Laín, S., J. L. Riechmann, and J. A. García.** 1991. RNA helicase: a novel activity associated with a protein encoded by a positive strand RNA virus. Nucleic Acids Res. **18**:7003–7006.
12. **Laín, S., J. L. Riechmann, M. T. Martín, and J. A. García.** 1989. Homologous potyvirus and flavivirus proteins belonging to a

superfamily of helicase-like proteins. Gene **82:**357–362.
13. **Linder, P., P. F. Lasko, P. Leroy, P. J. Nielsen, K. Nishi, J. Schnier, and P. P. Slonimski.** 1989. Birth of the D-E-A-D box. Nature (London) **337:**121–122.
14. **Lohman, T. M.** 1992. *Escherichia coli* DNA helicases: mechanisms of DNA unwinding. Mol. Microbiol. **6:**5–14.
15. **Maniatis, T., E. F. Fritsch, and J. Sambrook.** 1982. Molecular cloning: a laboratory manual. Cold Spring Harbor Laboratory, Cold Spring Harbor, N.Y.
16. **Matson, S. W., and K. A. Kaiser-Rogers.** 1990. DNA helicases. Annu. Rev. Biochem. **59:**289–329.
17. **Nishi, K., F. Morel-Deville, J. W. B. Hershey, T. Leighton, and J. Schnier.** 1988. An eIF-4A-like protein is a suppressor of an *Escherichia coli* mutant defective in 50S ribosomal subunit assembly. Nature (London) **336:**496–498.
18. **Rosenfeld, S. J., K. Yoshimoto, S. Kajigaya, N. S. Young, P. Warrener, G. Bansal, and M. S. Collett.** 1992. The region unique to the minor capsid protein of human parvovirus B19 is exposed on the virion surface. J. Clin. Invest. **89:**2023–2029.
19. **Rozen, F., I. Edery, K. Meerovitch, T. E. Dever, W. C. Merrick, and N. Sonenberg.** 1990. Bidirectional RNA helicase activity of eucaryotic translation initiation factors 4A and 4F. Mol. Cell. Biol. **10:**1134–1144.
20. **Scheffner, M., R. Knippers, and H. Stahl.** 1989. RNA unwinding activity of SV40 large T antigen. Cell **57:**955–963.
21. **Scheffner, M., R. Knippers, and H. Stahl.** 1991. Simian virus 40 large T antigen-catalyzed DNA and RNA unwinding reaction. Eur. J. Biochem. **195:**49–54.
22. **Schmid, S. R., and P. Linder.** 1992. D-E-A-D protein family of putative RNA helicases. Mol. Microbiol. **6:**283–292.
23. **Schwer, B., and C. Guthrie.** 1991. PRP16 is an RNA-dependent ATPase that interacts transiently with the spliceosome. Nature (London) **349:**494–499.
24. **Tamura, J. K., and M. Gellert.** 1990. Characterization of the ATP binding site on *Escherichia coli* DNA gyrase. J. Biol. Chem. **265:**21342–21349.
25. **Tamura, J. K., P. Warrener, and M. S. Collett.** RNA-stimulated NTPase activity associated with the p80 protein of the pestivirus bovine viral diarrhea virus. Virology, in press.
26. **Wassarman, D. A., and J. A. Steitz.** 1991. Alive with DEAD proteins. Nature (London) **349:**463–464.
27. **Wengler, G., and G. Wengler.** 1991. The carboxy-terminal part of the NS3 protein of the West Nile flavivirus can be isolated as a soluble protein after proteolytic cleavage and represents an RNA-stimulated NTPase. Virology **184:**707–715.